Neurobiology of Aging 95 (2020) 143–153

Contents lists available at ScienceDirect

Neurobiology of Aging

journal homepage: www.elsevier.com/locate/neuaging

Blood and cerebrospinal fluid neurofilament light differentially detect neurodegeneration in early Alzheimer's disease

Emelie Andersson[a,*], Shorena Janelidze[a], Björn Lampinen[b], Markus Nilsson[c], Antoine Leuzy[a], Erik Stomrud[a,d], Kaj Blennow[e,f], Henrik Zetterberg[e,f,g,h], Oskar Hansson[a,d,**]

[a] Clinical Memory Research Unit, Department of Clinical Sciences, Malmö, Lund University, Lund, Sweden
[b] Clinical Sciences Lund, Department of Medical Radiation Physics, Lund University, Lund, Sweden
[c] Clinical Sciences Lund, Department of Radiology, Lund University, Lund, Sweden
[d] Memory Clinic, Skåne University Hospital, Malmö, Sweden
[e] Department of Psychiatry and Neurochemistry, Institute of Neuroscience and Physiology, Sahlgrenska Academy, University of Gothenburg, Mölndal, Sweden
[f] Clinical Neurochemistry Laboratory, Sahlgrenska University Hospital, Mölndal, Sweden
[g] Department of Neurodegenerative Disease, UCL Queen Square Institute of Neurology, London, UK
[h] UK Dementia Research Institute at UCL, London, UK

ARTICLE INFO

Article history:
Received 17 December 2019
Received in revised form 16 July 2020
Accepted 19 July 2020
Available online 25 July 2020

Keywords:
Alzheimer's disease
Biomarker
Blood
Cerebrospinal fluid
Imaging
Neurofilament light

ABSTRACT

Cerebrospinal fluid (CSF) neurofilament light (NfL) concentration has reproducibly been shown to reflect neurodegeneration in brain disorders, including Alzheimer's disease (AD). NfL concentration in blood correlates with the corresponding CSF levels, but few studies have directly compared the reliability of these 2 markers in sporadic AD. Herein, we measured plasma and CSF concentrations of NfL in 478 cognitively unimpaired (CU) subjects, 227 patients with mild cognitive impairment, and 113 patients with AD dementia. We found that the concentration of NfL in CSF, but not in plasma, was increased in response to Aβ pathology in CU subjects. Both CSF and plasma NfL concentrations were increased in patients with mild cognitive impairment and AD dementia. Furthermore, only NfL in CSF was associated with reduced white matter microstructure in CU subjects. Finally, in a transgenic mouse model of AD, CSF NfL increased before serum NfL in response to the development of Aβ pathology. In conclusion, NfL in CSF may be a more reliable biomarker of neurodegeneration than NfL in blood in preclinical sporadic AD.

1. Introduction

During the past decade, several imaging and cerebrospinal fluid (CSF) biomarkers that reflect the neuropathological characteristics of Alzheimer's disease (AD), including extracellular deposition of aggregated beta-amyloid (Aβ), formation of intraneuronal neurofibrillary tangles composed of hyperphosphorylated tau, and neuronal loss, have been established (Blennow and Zetterberg, 2018; Laforce et al., 2018). These advances have made it possible to detect pathological processes in the preclinical stage of AD, before the manifestation of cognitive symptoms (Gustafson et al., 2007; Skoog et al., 2003; Stomrud et al., 2007). In recent years, the search for inexpensive and easily accessible blood-based biomarkers for monitoring of early pathological events and disease progression has intensified, given the invasiveness of lumbar puncture for CSF collection and the high cost and limited availability of positron emission tomography (PET) imaging biomarkers (Hampel et al., 2018).

Neurofilament light (NfL), an intermediate filament protein expressed exclusively in neurons, has emerged as a promising blood-based biomarker of neurodegeneration in several neurological disorders, including AD (Khalil et al., 2018). The protein is particularly abundant in large myelinated axons, where it plays essential roles for radial growth, structural stability, and effective conduction of nerve impulses (Sakaguchi et al., 1993; Zhu et al., 1997). Under normal physiological conditions, NfL is released into the interstitial fluid from where it reaches the CSF as well as the circulatory system. However, upon neuronal injury and loss, the

* Corresponding author at: Clinical Memory Research Unit, Department of Clinical Sciences, Malmö, Lund University, 221 84 Lund, Sweden.
** Corresponding author at: Memory Clinic, Skåne University Hospital, 20502 Malmö, Sweden. Tel.: +46 40 335036; fax: +46 40 335657.
E-mail addresses: emelie.andersson@med.lu.se (E. Andersson), oskar.hansson@med.lu.se (O. Hansson).

0197-4580/
https://doi.org/10.1016/j.neurobiolaging.2020.07.018

amount that reaches these fluid compartments is markedly elevated (Yuan et al., 2017). In sporadic AD, the concentrations of NfL in CSF and blood are significantly increased in both the prodromal and dementia stages of the disease, in which they associate with cognitive decline and disease-related structural brain changes (Mattsson et al., 2017; Zetterberg et al., 2016). Increased NfL concentration in CSF has also been reported in preclinical sporadic AD (Bos et al., 2019; Pereira et al., 2017), but similar studies on NfL in blood have not been able to show such changes at this early disease stage (Chatterjee et al., 2018; Mattsson et al., 2017). This suggests that NfL in CSF might be a more reliable biomarker of neurodegenerative processes in preclinical sporadic AD than NfL in blood. However, a direct comparison between the performance of NfL in CSF and blood in different stages of the disease is largely unexplored in samples derived from the same study population.

Well-characterized mouse models with a biomarker profile similar to that in humans hold great translational value in AD research. In accordance with clinical findings, experimental studies using transgenic (tg) mouse models of Aβ pathology and other proteinopathies have shown marked age-dependent increases of NfL concentration in both CSF and blood. These changes are also responsive to inhibition of pathological processes (Bacioglu et al., 2016). However, changes in NfL concentration in CSF compared to blood in relation to AD-related pathology over time have not been thoroughly investigated in mouse models of the disease. This knowledge would be valuable for future studies on underlying disease mechanisms and treatment response to novel disease-modifying drugs.

Herein, we measured the concentrations of NfL in CSF and plasma in a cohort derived from the Swedish BioFINDER study consisting of cognitively unimpaired (CU) subjects ($n = 478$), patients with mild cognitive impairment (MCI; $n = 227$), and patients with AD dementia ($n = 113$). In addition, we determined the concentrations of NfL in CSF and serum collected at different time points from the 5×FAD tg mouse model of AD ($n = 40$) and age-matched non-tg littermates ($n = 41$). We tested the hypothesis that NfL concentrations are increased at an earlier disease stage in CSF than in plasma when assessed in CU subjects, patients with MCI, and patients with AD dementia, all categorized based on CSF Aβ and neurodegeneration status. Furthermore, we studied whether NfL concentrations in CSF were associated with cerebral Aβ deposition (^{18}F-flutemetamol PET) and metrics of white matter microstructure from diffusion tensor imaging (DTI) at an earlier disease stage compared to those in plasma. Finally, we studied whether the concentration of NfL in CSF was increased at an earlier time point than in serum in 5×FAD mice, and if the association with cerebral amyloid plaque load was stronger for NfL in CSF than in serum in this mouse model.

2. Materials and methods

2.1. BioFINDER study population

The study was approved by the Regional Ethics Committee in Lund, Sweden, and the participants or their relatives gave written informed consent.

The study population originated from the prospective and longitudinal Swedish BioFINDER study and consisted of 298 cognitively healthy elderly participants, 407 patients with mild cognitive symptoms, and 113 patients with AD dementia from which baseline CSF and plasma NFL samples were available.

Cognitively healthy elderly participants were recruited from the longitudinal population-based Malmö Diet and Cancer Study between 2010 and 2014 according to the following inclusion criteria: ≥60 years of age, absence of cognitive symptoms as assessed by a physician, Mini-Mental State Examination score of 28–30 at screening visit, not fulfilling the criteria for MCI or any dementia, and fluency in Swedish. Exclusion criteria were significant neurological or psychiatric illness, significant alcohol or substance abuse, and refusing lumbar puncture or magnetic resonance imaging (MRI).

Patients with mild cognitive symptoms were consecutively enrolled from the Memory Clinic at Skåne University Hospital and Ängelholm Hospital in Sweden between 2010 and 2014. Included individuals had an age between 60 and 80 years, were referred to any of the 2 memory clinics due to cognitive symptoms, had an Mini-Mental State Examination score of 24–30 at baseline visit, did not fulfill the criteria for any dementia, and were fluent in Swedish. The exclusion criteria were cognitive impairment that with certainty could be explained by another condition or disease, significant alcohol or substance abuse, and refusing lumbar puncture or neuropsychological assessment. Following neuropsychological assessment including a test battery evaluating verbal ability, episodic memory function, visuospatial construction ability, and attention and executive functions, 180 patients were classified as subjective cognitive decline and 227 patients were classified as MCI. In accordance with the guidelines from the US National Institute on Aging-Alzheimer's Association (Jack et al., 2018), cognitively healthy elderly participants and patients with subjective cognitive decline were included in the CU group.

Patients with AD dementia were included after thorough clinical assessment at the Memory Clinic at Skåne University Hospital in Sweden. All study participants met the criteria for probable AD dementia as defined by the National Institute of Neurological and Communicative Disorders and Stroke and the Alzheimer's Disease and Related Disorders Association (Mckhann et al., 2011). Individuals with significant alcohol or substance abuse were excluded.

Study participants who were CU or diagnosed with MCI were categorized into groups with normal (A−) or pathologic (A+) CSF Aβ using the Aβ42/Aβ40 ratio with the cutoff <0.091. This cutoff was established using Gaussian mixture modeling. In addition, these individuals were further categorized based on normal (N−) and abnormal (N+) cortical thickness in AD-susceptible temporal regions as determined by MRI (see Section 2.3 below) with the cutoff <2.25. As cortical thickness was not bimodally distributed, Gaussian mixture modeling for cutoff determination could not be applied. Instead, the cutoff was defined as mean −1.5 standard deviation of A− CU cases, which has been commonly used in other studies. Participants with AD dementia were all A+, however, no information on cortical thickness was available for this group.

2.2. CSF and blood collection in the BioFINDER study population

Collection of lumbar CSF and blood samples from each study participant was performed on the same day, where blood was obtained within 15 minutes of CSF sampling. Lumbar CSF samples were collected according to a standardized protocol (Blennow et al., 2010), centrifuged for 10 minutes at 2000×g at 4 °C, and aliquoted into polypropylene tubes. Blood was drawn into EDTA-containing tubes and centrifuged for 10 minutes at 2000×g at 4 °C. Following centrifugation, plasma was collected and aliquoted into polypropylene tubes. The obtained CSF and plasma samples were stored at −80 °C until biochemically analyzed.

2.3. Magnetic resonance imaging

MRI was completed in 478 CU subjects and 227 MCI patients, and the average time interval between MRI acquisition and fluid collection was 17 days. High-resolution T1-weighted MP-RAGE (TR = 1950 ms, TE = 3.4 ms, in-plane resolution = 1 × 1 mm^2, slice thickness = 1.2 mm, 176 slices) and transversal T2-weighted

FLAIR (TR = 9000 ms, TE = 89 ms, TI = 2500 ms, voxel size 0.7 × 0.7 × 4 mm^3, distance factor 25%, 27 slices) imaging was performed on a 3T MR scanner (Siemens Tim Trio 3T; Siemens Medical Solutions, Erlangen, Germany).

Cortical reconstruction and volumetric segmentation were performed with the FreeSurfer image analysis pipeline v5.3 (http://surfer.nmr.mgh.harvard.edu/). Briefly, the T1-weighted images underwent correction for intensity homogeneity, removal of non-brain tissue, and segmentation into gray matter and white matter with intensity gradient and connectivity among voxels. Cortical modeling allowed parcellation of the cerebral cortex into units with respect to gyral and sulcal structure (Desikan et al., 2006). Cortical thickness was measured as the distance from the gray/white matter boundary to the corresponding pial surface. Reconstructed data sets were visually inspected for accuracy, and segmentation errors were corrected. To determine AD-related brain atrophy we used the average cortical thickness in a predefined temporal lobe meta-region (composed of entorhinal, inferior temporal, middle temporal, and fusiform cortex) (Jack et al., 2017).

Global white matter lesion volume was determined by the use of an automated segmentation method, using the lesion prediction algorithm in the LST toolbox implemented in SPM8 (Schmidt et al., 2012).

For diffusion MRI, a single-shot EPI sequence was used to obtain 66 contiguous axial slices with a spatial resolution of 2 × 2 × 2 mm^3 (TR/TE = 86/8200 ms). The diffusion encoding was performed in 64 directions with b = 1000 s/mm^2, and one additional volume was obtained for b = 0 s/mm^2. To correct for motion and eddy-current induced distortions, all data were registered to the b = 0 s/mm^2 volume using an affine transform implemented in Elastix (Klein et al., 2010). DTI (Basser et al., 1994) analysis was performed using linear least squares with heteroscedasticity correction with software developed in-house in MATLAB (The MathWorks Inc, Natick, MA). Parameter maps for mean diffusivity (MD) and fractional anisotropy (FA) were calculated from the diffusion tensor.

The DTI data were analyzed using tract-based spatial statistics (TBSS) (v 1.03) from the FMRIB Software Library (Smith et al., 2006). In this process, FA volumes were first masked with the FSL Brain Extraction Tool and then non-linearly registered to the 1 mm^3 FMRIB58 FA template in MNI152 standard space, using FLIRT and FNIRT (Andersson et al., 2007). The resulting subject-specific non-linear transform was then applied to the MD map. The maps in template space were then skeletonized by computing of the projection of the FA map onto the FMRIB58 template skeleton. Statistical processing was performed using a significance threshold of 0.05 in Threshold-Free Cluster Enhancement and FSL Randomize (v 2.9), with 7500 permutations for generation of the null distribution. When generating the p-maps, multiple comparison-correction was accounted for by controlling the family-wise error rate. Hypothesis tests were performed using the null hypothesis that the regression coefficient for CSF NfL, or for plasma NfL, was zero, using age and sex as additional covariates. The tests were performed separately for CSF NfL and for plasma NfL for each of the 3 groups comprising all subjects, those in the CU group, or those in the MCI group. Due to incomplete data or failure of normalization, 11 CU subjects and 5 MCI subjects were excluded from the TBSS analysis.

2.4. ^{18}F-flutemetamol PET imaging

^{18}F-flutemetomol PET scans for visualization of cerebral Aβ depositions were completed for 382 individuals, including 244 CU subjects and 138 MCI patients. Production of ^{18}F-flutemetamol was performed at the radiopharmaceutical production site in Risø, Denmark, using a FASTlab synthesizer module (GE Healthcare, Cleveland, OH). PET/CT scans of the brain were obtained from 2 different sites using the same type of scanner (Germini; Philips Healthcare, Best, Netherlands). ^{18}F-flutemetamol summation images for the period 90–110 minutes post injection a single dose of ^{18}F-flutemetamol was analyzed using the NeuroMarQ software (GE Healthcare). A volume of interest (VOI) template was applied to define a global neocortical composite region, encompassing prefrontal, parietal, temporal lateral, anterior cingulate, posterior cingulate, and precuneus VOIs (Lundqvist et al., 2013). The standardized uptake value ratio was defined as the uptake in a VOI normalized to a composite reference region (whole cerebellum, the pons/brainstem, and eroded cortical white matter).

2.5. Animals

Two- to 12-month-old male and female heterozygous 5×FAD tg mice (n = 40), originally obtained from Jackson Laboratory, and age-matched non-tg littermates (n = 41) were used for the experiments. Animals were housed in groups of 2–6 mice per cage under a 12:12 hour light/dark cycle with free access to food and water. Under the control of the mouse Thy1 promotor element, 5×FAD mice overexpress human APP(695) with the K670N/M671L (Swedish), 1716V (Florida), and V7171 (London) mutations together with human PS1 harboring the M146L and L286V mutations. Intraneuronal Aβ appears at 1.5 months in the deep cortical layers and subiculum, and extracellular amyloid plaques start to accumulate in the same regions around 2 months of age, spreading to other brain areas as the animal ages. In addition, a reduction in pre- and postsynaptic markers as well as neuronal loss has been reported in 9-month-old mice (Oakley et al., 2006).

The experimental procedures were carried out in accordance with the Swedish animal research regulations and were approved by the committee of animal research at Lund University (ethical permit number: 7482/2017).

2.6. CSF, blood, and brain tissue collection in mice

CSF was collected from cisterna magna in accordance with a method previously described (Liu and Duff, 2008). All sample collection was performed between 9 AM and 13 PM. Under isoflurane anesthesia, mice were placed on a stereotaxic instrument and an incision of the skin inferior to the occiput was made. Using a dissecting microscope, the underlying neck muscles were then separated to expose the dura mater of the cisterna magna. A glass capillary tube with a tapered tip was used to penetrate the dura mater and collect CSF. Samples were immediately transferred to protein LoBind tubes (Eppendorf, Hamburg, Germany), snap frozen on dry ice, and stored at −80 °C until analysis.

Following CSF sampling, blood was collected from the left heart ventricle using a 23G needle and immediately transferred to protein LoBind Tubes (Eppendorf). The blood samples were allowed to clot for 2 hours at room temperature before they were centrifuged at 2000×g for 20 minutes. Serum was then collected, aliquoted into protein LoBind tubes (Eppendorf), and stored at −80 °C until analysis.

For brain tissue collections, mice were transcardially perfused with ice-cold 0.1 M phosphate buffer (PB). The brain was removed and the left hemisphere was fixed in 4% paraformaldehyde in 0.1 M PB, pH 7.4, for 48 hours at 4 °C and then immersed in 30% sucrose solution for 48 hours at 4 °C. Brains were serially cut into 30 μm sagittal sections using a sliding microtome (Leica Biosystems, Wetzlar, Germany) and collected in antifreeze solution (30% sucrose and 30% ethylene glycol in PB) for storage at −20 °C.

2.7. Thioflavin S staining and analysis of mouse brain sections

Free-floating sagittal brain sections (30 μm) were washed 3 × 10 minutes in Tris-buffered saline and then stained with 0.01% Thioflavin S (ThioS) in 50% ethanol for 10 minutes. Sections were washed 2 × 1 minute in 50% ethanol, 3 × 1 minute in ddH_2O, and finally 10 minutes in Tris-buffered saline. The stained specimens were mounted on glass slides and coverslipped with SlowFade Gold Antifade Mountant (Life Technologies, Carlsbad, CA) according to the manufacturer's recommendations. Images of cortex and subiculum from 3 sections per animal were captured using a 10× objective lens on an Olympus IX70 fluorescence microscope equipped with a Hamamatsu ORCA-Flash4.0 LT+ digital COMOS camera. The area (%) covered by ThioS-positive amyloid plaques in the regions of interest was quantified using the Fiji software by applying an automated threshold that was maintained for all images analyzed.

2.8. Biochemical analysis of CSF and blood from the BioFINDER study population and mice

CSF NfL concentration in the BioFINDER study population was measured using a sensitive sandwich ELISA method (NF-light ELISA kit; UmanDiagnostics AB, Umeå, Sweden). Intra-assay coefficient of variance (CV) ranged between 7% and 10% and inter-assay CV was 13%. An in-house Simoa NfL assay, in which the monoclonal antibodies and calibrators from the NF-light ELISA kit (UmanDiagnostics AB) were transferred onto the Simoa platform using a homebrew kit (Quanterix, Lexington, MA), was used to measure plasma NfL concentration in the BioFINDER study population, as well as CSF and serum NfL concentrations in mice. The core domain of NfL, against which the antibodies are directed, is fully conserved between humans and mice (Lee et al., 1986). For measurement of plasma samples from the BioFINDER study population, the intra-assay CV was 5.5% and the inter-assay CV was 8.2% for the low-concentration quality control sample (11.1 pg/mL). For the high-concentration quality control sample (107.0 pg/mL), the corresponding CVs were 9.3% and 9.4%, respectively. Intra-assay CV for measurement of mouse CSF samples ranged between 2.9% and 11.1%, and intra- and inter-assay CV for measurement of mouse serum samples ranged between 3.2% and 8.7% and 6.5% and 13.8%, respectively. The concentration of Aβ40, Aβ42, and phosphorylated tau in CSF in the BioFINDER study population was measured by Euroimmun immunoassay. All measurements were performed in one round of experiments using one batch of reagents by board-certified laboratory technicians who were blinded to clinical and genotype information.

2.9. Statistical analysis

For the BioFINDER study population, demographic factors and clinical characteristics were compared between different diagnostic groups using the Mann-Whitney *U*-test for continuous variables and the χ^2 test for categorical variables. Group comparisons of CSF and plasma biomarkers were performed on log-transformed data using univariate general linear models adjusted for the confounding effects of age and sex. *p*-values were corrected for multiple comparisons using the Bonferroni method. Spearman's rank-ordered correlation coefficient and linear regression models adjusted for age and sex were used to examine associations between 2 continuous variables. The diagnostic accuracy of NfL in CSF and plasma was evaluated using receiver operating characteristic curve analysis by calculating the area under the curve (AUC). Associations between NfL concentrations and ^{18}F-flutemetamol standardized uptake value ratio were analyzed voxel-wise using SPM12 multilinear regression models, including age, sex, and the time interval between fluid collection and ^{18}F-flutemetamol PET acquisition as covariates. Parametric maps were adjusted for multiple comparisons using family wise error correction.

Nonparametric statistical methods were used for analysis of data derived from animal experiments due to the relatively small sample size. Three extreme outliers with CSF or plasma NfL concentrations above 3 interquartile ranges of the third quartile were excluded from the analysis. The Jonckheere-Terpstra trend test was performed to study if CSF and serum NfL concentrations increased with age in 5×FAD mice and non-tg littermates. This test was also used to study if amyloid plaque load in cortex and subiculum of 5×FAD mice increased with age. If a statistically significant trend was found, post hoc analysis for group comparisons between the youngest group an all other groups were performed using the Mann-Whitney *U*-test. *p*-values were corrected for multiple comparisons using the Bonferroni method. In addition, the Mann-Whitney *U*-test was performed to compare the concentrations of NfL in CSF and serum between 5×FAD mice and age-matched non-tg littermates. Correlation analysis was done using Spearman's rank-ordered correlation coefficient. For comparisons between correlation coefficients, Meng's *Z*-test for correlated correlations was performed (Meng et al., 1992). Statistical analysis was performed using IBM SPSS Statistics 25 and corresponding graphs were produced in GraphPad Prism 8.

3. Results

3.1. CSF and plasma NfL concentrations and demographic factors

Demographic factors and biomarker characteristics for the BioFINDER study population are listed in Table 1 and Supplementary Table 1. CSF and plasma NfL concentrations correlated significantly with age in the whole study population ($r_{s\ (CSF)} = 0.32$, $p < 0.001$; $r_{s\ (plasma)} = 0.44$, $p < 0.001$), as well as in CU subjects ($r_{s\ (CSF)} = 0.39$, $p < 0.001$; $r_{s\ (plasma)} = 0.49$, $p < 0.001$), patients with MCI ($r_{s\ (CSF)} = 0.23$, $p < 0.001$; $r_{s\ (plasma)} = 0.28$, $p < 0.001$), and patients with AD dementia ($r_{s\ (CSF)} = 0.21$, $p < 0.05$; $r_{s\ (plasma)} = 0.38$, $p < 0.001$). In the whole study population, men had significantly higher CSF NfL concentration than women ($p < 0.001$). Similar results were observed in CU subjects ($p < 0.001$), patients with MCI ($p < 0.001$), and patients with AD dementia ($p < 0.05$). No sex differences in plasma NfL concentration were found.

3.2. Correlation between NfL concentrations in CSF and plasma

Spearman correlation analysis revealed a positive correlation between plasma and CSF NfL concentrations when measured in the whole study population ($r_s = 0.58$, $p < 0.001$) as well as in CU subjects ($r_s = 0.48$, $p < 0.001$), patients with MCI ($r_s = 0.50$, $p < 0.001$), and patients with AD dementia ($r_s = 0.53$, $p < 0.001$) (Supplementary Fig. 1). Similar associations were found when adjusting for the confounding effects of age and sex using linear regression models (whole study population, $\beta = 0.51$, $p < 0.001$; CU, $\beta = 0.36$, $p < 0.001$; MCI, $\beta = 0.55$, $p < 0.001$; AD dementia, $\beta = 0.51$, $p < 0.001$).

3.3. CSF and plasma NfL concentrations in diagnostic groups stratified by A/N status

CSF and plasma NfL concentrations were significantly higher in patients with MCI ($p < 0.00033$) and AD dementia ($p < 0.00033$) when compared to CU subjects (Table 1). When the diagnostic groups were further categorized based on CSF Aβ status (A− or A+) and neurodegeneration (N− or N+), CU subjects characterized as

Table 1
Demographic and baseline information on the study participants

	CU ($n = 478$)	MCI ($n = 227$)	AD ($n = 113$)
Age (y)	72.1 (5.5)	70.6 (5.4)[a]	75.0 (7.2)[b,c]
Sex (% female)	58.2	40.5[b]	63.7[c]
Education level (y)	12.3 (3.7)	11.1 (3.3) ($n = 223$)[b]	9.6 (2.8) ($n = 71$)[b,d]
APOE ε4 (% positive)	32.4 ($n = 477$)	52.0[b]	66.3 ($n = 110$)[b,e]
MMSE score	28.9 (1.2)	27.1 (1.8)[b]	21.7 (3.7)[b,c]
^{18}F-Flutemetamol, global (SUVR)	0.73 (0.15) ($n = 259$)	0.90 (0.21) ($n = 143$)[f]	N/A
CSF NfL (pg/mL)	992 (612)	1528 (1308)[b]	1827 (1591)[b]
Plasma NfL (pg/mL)	23 (34)	28 (23)[b]	42 (26)[b,c]
CSF Aβ42/40 ratio	0.11 (0.037)	0.090 (0.041)[b]	0.055 (0.016)[b,c]
CSF t-tau (pg/mL)	337 (141)	437 (218)[b]	653 (234)[b,c]
CSF p-tau (pg/mL)	49 (31) ($n = 458$)	79 (51) ($n = 218$)[b]	124 (50) ($n = 111$)[b,c]

Continuous data are presented as mean (SD). Mann-Whitney *U*-test and χ^2 test were used to compare demographic factors and clinical characteristics between the groups. Group comparisons of CSF and plasma biomarkers (log-transformed) were performed using univariate general linear models adjusted for age and sex. *p*-values were corrected for multiple comparisons using the Bonferroni method.
Key: Aβ, beta amyloid; AD, Alzheimer's disease; CSF, cerebrospinal fluid; CU, cognitively unimpaired; MCI, mild cognitive impairment; MMSE, Mini-Mental State Examination; N/A, not applicable; NfL, neurofilament light; p-tau, phosphorylated tau; t-tau, total tau.
[a] $p < 0.017$ versus CU.
[b] $p < 0.00033$ versus CU.
[c] $p < 0.00033$ versus MCI.
[d] $p < 0.0033$ versus MCI.
[e] $p < 0.017$ versus MCI.
[f] $p < 0.001$ versus CU.

A+N− and A+N+ had significantly higher concentrations of NfL in CSF when compared to those characterized as A−N− (CU A+N−, $p < 0.00125$; CU A+N+, $p < 0.00125$). More specifically, the mean NfL concentration in CSF was 1.28-fold higher in A+N− CU subjects and 1.66-fold higher in A+N+ CU subjects. Plasma NfL concentration, on the other hand, was not significantly increased in CU subjects with Aβ pathology (A+) or evidence of neurodegeneration (N+), although the mean plasma NfL concentration was 1.40-fold higher in A+N− CU subjects and 1.60-fold higher in A+N+ CU subjects when compared to CU subjects categorized as A−N−. Significantly higher NfL concentrations in CSF were also found in MCI patients characterized as A−N− ($p < 0.000125$), A+N− ($p < 0.000125$), A−N+ ($p < 0.000125$), and A+N+ ($p < 0.000125$), as well as in patients with AD dementia ($p < 0.000125$) when compared to A−N− CU subjects. Similar results were found for the concentration of NfL in plasma (MCI A−N−, $p < 0.00125$; MCI A+N−, $p < 0.000125$; MCI A−N+, $p < 0.000125$; MCI A+N+, $p < 0.000125$; AD dementia, $p < 0.000125$) (Table 2; Supplementary Fig. 2A and B). Furthermore, in Supplementary Table 2 we describe the AUCs of CSF and plasma NfL when distinguishing the different diagnostic groups. In brief, the AUCs were higher for CSF NfL compared with plasma NfL.

3.4. Associations between CSF and plasma NfL concentrations and ^{18}F-flutemetamol PET

Next, we studied whether CSF and plasma NfL concentrations were associated with the amount of cortical Aβ fibrils as measured with amyloid (^{18}F-flutemetamol) PET. In the whole study population, voxel-wise regression analysis revealed a significant association between CSF NfL concentration and the uptake of ^{18}F-flutemetamol, particularly in prefrontal, occipital, and temporal cortical areas, precuneus, and posterior cingulate cortex. In contrast, significant associations between plasma NfL concentration and ^{18}F-flutemetamol uptake were largely absent (Fig. 1A, Supplementary Fig. 3A). Similarly, in CU subjects, mainly CSF NfL was associated with the uptake of ^{18}F-flutemetamol (Fig. 1B), however, these results did not survive multiple comparison (Supplementary Fig. 3B). In patients with MCI, the uptake of ^{18}F-flutemetamol was not significantly associated with either CSF or plasma NfL concentrations (Fig. 1C, Supplementary Fig. 3C).

3.5. Association between CSF and plasma NfL concentrations and DTI metrics in TBSS

NfL concentrations in body fluids are thought to mainly reflect axonal degeneration (Yuan et al., 2017). Consequently, we next studied the associations between the concentrations of NfL in CSF and plasma with microstructural changes in subcortical white matter using DTI. Typically, FA decreases and MD increases with increasing white matter damage in neurodegenerative disorders (Horsfield and Jones, 2002). CSF NfL concentration associated negatively with FA and positively with MD across most of the TBSS white matter skeleton in the whole study population as well as in CU subjects and patients with MCI. Plasma NfL, on the other hand, was negatively associated with FA only among patients with MCI.

Table 2
CSF and plasma NfL concentrations in diagnostic groups stratified by A/N status

	CU				MCI				AD
	A−N− ($n = 300$)	A+N− ($n = 118$)	A−N+ ($n = 31$)	A+N+ ($n = 29$)	A−N− ($n = 68$)	A+N− ($n = 79$)	A−N+ ($n = 27$)	A+N+ ($n = 53$)	A+ ($n = 113$)
CSF NfL (pg/mL)	870 (437)	1112 (775)[a]	1292 (712)	1446 (864)[a]	1284 (1207)[b]	1292 (705)[b]	2238 (1803)[b]	1832 (1635)[b]	1827 (1591)[b]
Plasma NfL (pg/mL)	20 (10)	28 (66)	29 (19)	32 (18)	24 (17)[a]	27 (17)[b]	38 (48)[b]	30 (18)[b]	42 (26)[b]

Data are given as mean (SD). Univariate general linear models adjusted for age and sex were used for group comparisons. Statistical analysis was performed on log-transformed CSF and plasma NfL concentrations. *p*-values were corrected for multiple comparisons using the Bonferroni method.
Key: AD, Alzheimer's disease; CSF, cerebrospinal fluid; CU, cognitively unimpaired; MCI, mild cognitive impairment; NfL, neurofilament light; SD, standard deviation; SUVR, standardized uptake value ratio.
[a] $p < 0.00125$ versus CU A−N−.
[b] $p < 0.000125$ versus CU A−N−.

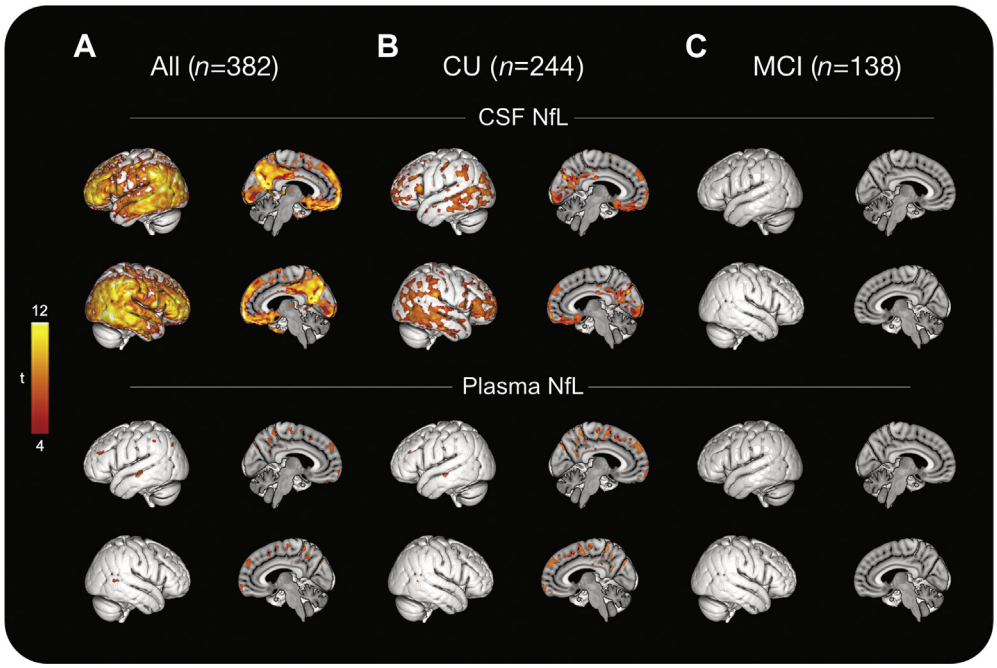

Fig. 1. Association between CSF and plasma NfL concentrations and ^{18}F-flutemetamol PET. Voxel-wise associations between ^{18}F-flutemetamol PET and NfL concentrations in CSF and plasma across the whole study population (A), CU subjects (B), and patients with MCI (C). Parametric maps were thresholded at $p < 0.001$ (uncorrected, cluster extent ≥100 voxels). All analysis was adjusted for age, sex, and time interval between fluid collection and ^{18}F-flutemetamol PET acquisitions. Abbreviations: CSF, cerebrospinal fluid; CU, cognitively unimpaired; MCI, mild cognitive impairment; NfL, neurofilament light; PET, positron emission tomography.

This association was less widespread compared to findings for NfL in CSF. No association between plasma NfL and MD was found either in the whole study population or when analyzed within the different diagnostic groups (Fig. 2A–C).

3.6. CSF and plasma NfL concentrations in 5×FAD mice and non-tg littermates

There was a significant positive correlation between CSF and serum NfL concentrations in both 5×FAD mice ($r_s = 0.67$, $p < 0.001$) and non-tg littermates ($r_s = 0.40$, $p < 0.01$) when measured over all age groups (Supplementary Fig. 4A and B). The Jonckheere-Terpstra test revealed a statistically significant trend of higher CSF and serum NfL concentrations with increased age in 5×FAD mice ($p_{CSF} < 0.001$; $p_{serum} < 0.001$). Similar results were observed for CSF NfL concentration in age-matched non-tg littermates ($p < 0.001$), whereas no significant increase in serum NfL concentration was found in these wild-type mice (Supplementary Table 3). When compared to age-matched non-tg littermates, 5×FAD mice had significantly higher concentrations of NfL in CSF at all assessed time points. Already at 2 months of age, the median CSF NfL concentration was elevated around 15-fold (Fig. 3A). In contrast, significant differences in the concentration of serum NfL were first observed from 4 months of age (Fig. 3B).

3.7. Association between CSF and plasma NfL concentrations and amyloid plaque load in 5×FAD mice

ThioS-positive amyloid plaques were observed in both the cortex and subiculum at 2 months of age in 5×FAD mice, and there was a significantly higher plaque load with increased age in the 2 regions ($p_{cortex} < 0.001$; Fig. 4A and B; $p_{subiculum} < 0.001$, Supplementary Fig. 5A and B). Both CSF and serum NfL concentration correlated with cortical plaque load when measured over all age groups ($r_{s\ (CSF)} = 0.76$, $p_{CSF} < 0.001$; $r_{s\ (serum)} = 0.58$, $p_{serum} < 0.001$; Fig. 4C and D). When comparing the 2 correlation coefficients, the correlation with cortical plaque load was significantly higher for CSF NfL concentration than for serum NfL concentration ($z = 1.97$, $p < 0.05$). In addition, CSF and serum NfL concentrations correlated with plaque load in the subiculum ($r_{s\ (CSF)} = 0.75$, $p_{CSF} < 0.001$; $r_{s\ (serum)} = 0.60$, $p_{serum} < 0.001$; Supplementary Fig. 5C and D), however, no significant difference between these correlations was found.

4. Discussion

In the present study, our main findings show that the concentration of NfL in CSF was significantly increased in CU subjects with Aβ pathology, whereas changes in plasma were first observed in patients with MCI. Furthermore, in CU subjects, the concentration of NfL in CSF was associated with accumulation of Aβ in the brain in a more widespread manner compared to NfL in plasma. We also found that the concentration of NfL in CSF, but not in plasma, was associated with compromised white matter microstructure in CU subjects. Supportive of these results, the concentration of NfL in both CSF and serum was increased and associated with disease progression in the 5×FAD mouse model of AD. In comparison to serum, the concentration of NfL in CSF was elevated at an earlier time point and showed a greater association with cortical amyloid plaque load. Together, these results suggest that NfL in CSF constitutes a more reliable biomarker of neuroaxonal pathological processes than NfL in blood in preclinical sporadic AD.

4.1. The concentration of NfL in CSF is significantly increased earlier than in blood

Consistent with previous observations (Mattsson et al., 2017), the concentration of NfL in plasma correlated positively with those

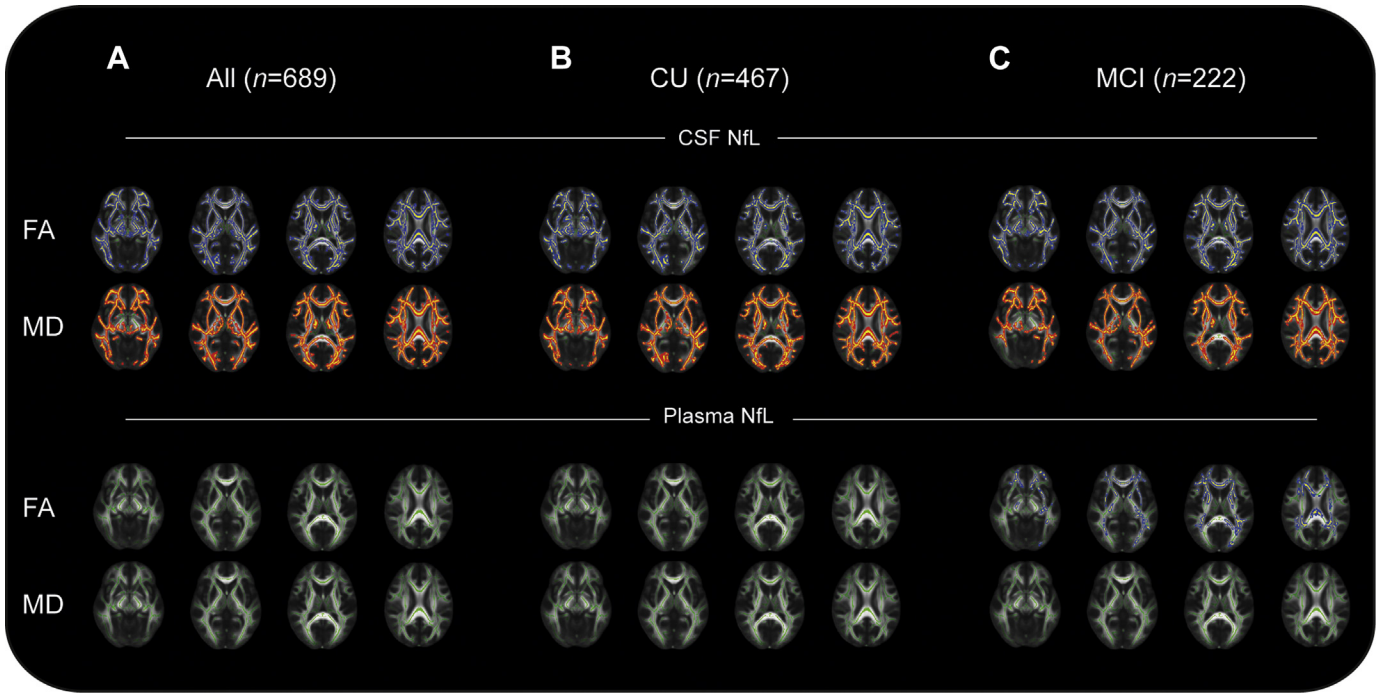

Fig. 2. Association between CSF and plasma NfL concentrations and DTI metrics. Associations between CSF and plasma NfL concentrations and FA and MD from DTI across the whole study population (A), CU subjects (B), and patients with MCI (C). NfL in CSF was negatively associated (blue) with FA and positively associated (red) with MD in all investigated groups. NfL in plasma was negatively associated with FA in patients with MCI, but with a smaller spatial extent compared with NfL in CSF. All analyses were adjusted for age and sex. Abbreviations: CSF, cerebrospinal fluid; CU, cognitively unimpaired; DTI, diffusion tensor imaging; FA, fractional anisotropy; MCI, mild cognitive impairment; MD, mean diffusivity; NfL, neurofilament light. (For interpretation of the references to color in this figure legend, the reader is referred to the Web version of this article.)

in CSF in the whole study population, as well as in the different diagnostic groups, suggesting that NfL in blood is likely to originate from the central nervous system (CNS). In addition, NfL in both CSF and plasma were higher in patients with MCI and AD dementia compared to CU subjects, as reported by others (Mattsson et al., 2017, 2019; Olsson et al., 2019; Zetterberg et al., 2016), suggesting that NfL tracks neurodegeneration. When the diagnostic groups were further categorized based on A/N status, increased concentration of NfL in CSF was found already in A+N− and A+N+ CU subjects, whereas significant changes in plasma NfL were only found in patients with MCI and AD dementia. This may to some extent be due to higher variability in the concentration of NfL in plasma than in CSF across individuals, given that the fold change of the mean NfL concentration in A+N− and A+N+ CU subjects with respect to that in A−N− CU subjects was similar in plasma and CSF. Indeed, several physiological confounding factors may influence the accuracy of the measurement of NfL in blood compared to CSF, such as lower concentrations as a result of the larger volume of blood compared to CSF, degradation in the blood or liver, matrix effects, and renal clearance (Hampel et al., 2018). Furthermore, although

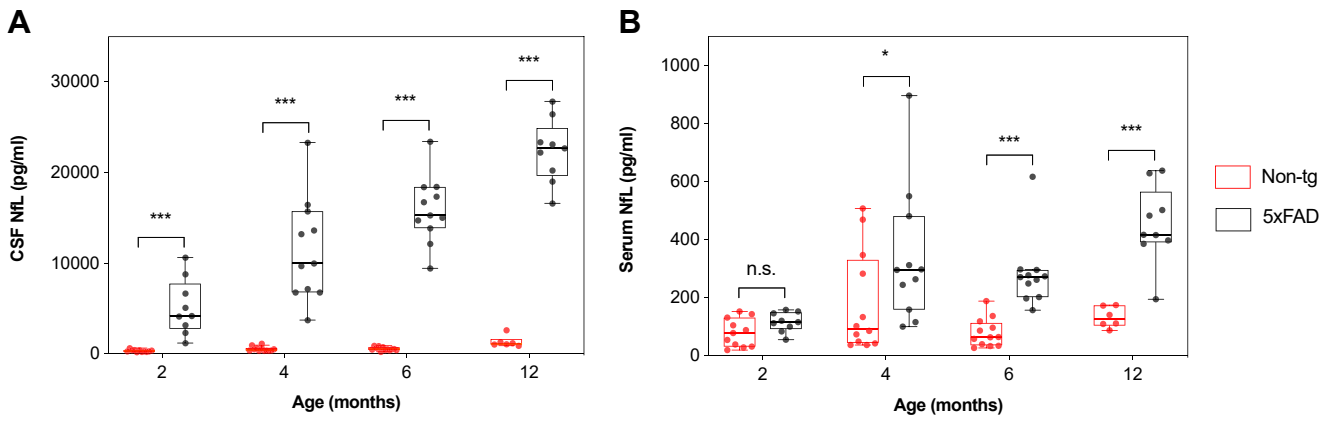

Fig. 3. CSF and serum NfL concentrations in 5×FAD mice and non-tg littermates. The concentration of NfL in CSF and serum was measured in 5×FAD mice and age-matched non-tg littermates at 2 (5×FAD: $n = 9$; non-tg: $n = 11$), 4 (5×FAD: $n = 11$; non-tg: $n = 12$), 6 (5×FAD: $n = 11$; non-tg: $n = 12$), and 12 (5×FAD: $n = 9$; non-tg: $n = 6$) months of age. (A) CSF NfL concentration in 5×FAD mice was significantly higher than those in age-matched non-tg littermates at all assessed time points. (B) Serum NfL concentration in 5×FAD mice was significantly higher than those in age-matched non-tg littermates at 4, 6, and 12 months of age. Data are presented as median and IQR. Whiskers represent data within 1.5 IQR of the lower and upper quartiles. Statistical analysis for comparison between 5×FAD mice and age-matched non-tg littermates was performed using the Mann-Whitney *U*-test (*$p < 0.05$, ***$p < 0.001$). Abbreviations: CSF, cerebrospinal fluid; IQR, interquartile range; NfL, neurofilament light.

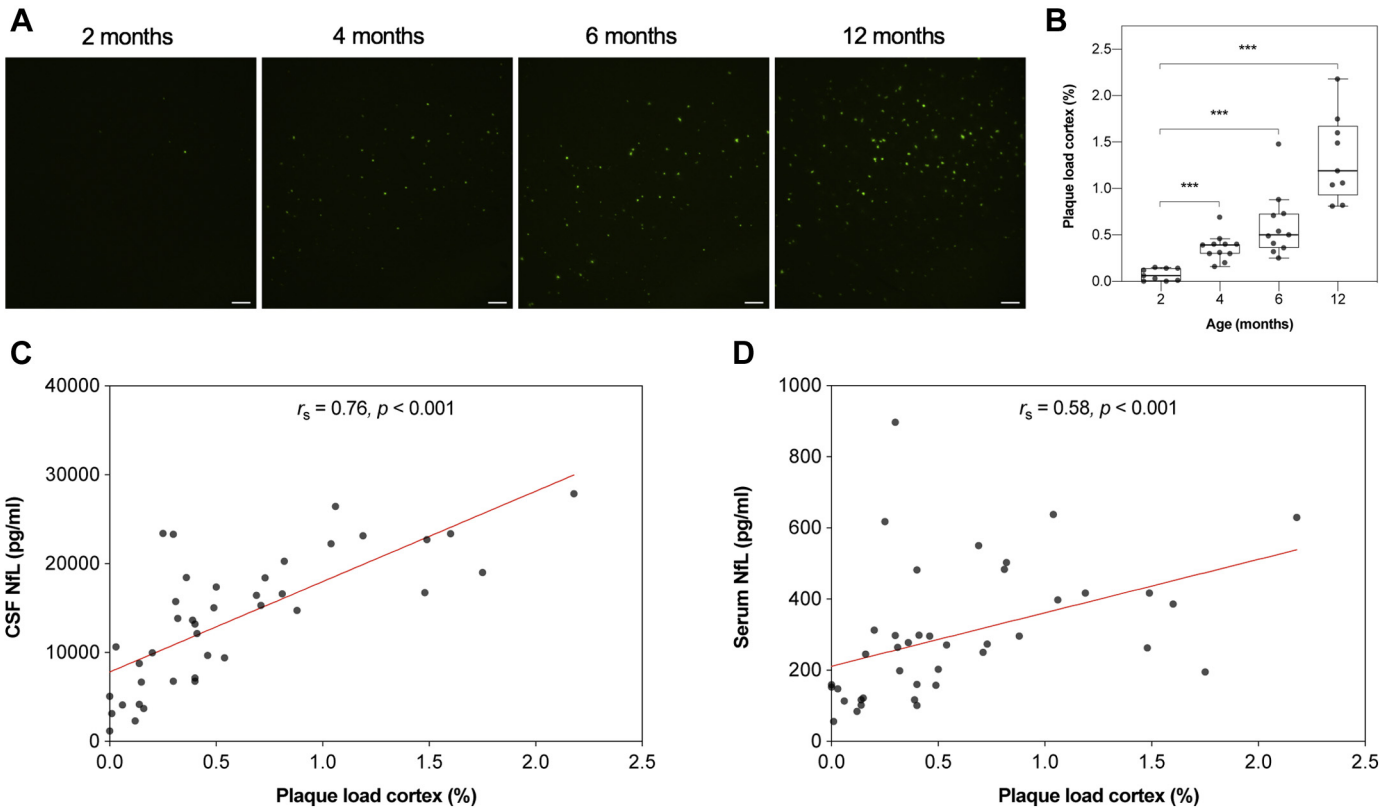

Fig. 4. Cortical amyloid plaque load and its correlation to CSF and serum NfL concentrations in 5×FAD mice. (A) Representative images of ThioS-positive amyloid plaques in cortex of 2 ($n = 9$), 4 ($n = 11$), 6 ($n = 11$), and 12 ($n = 9$) months old 5×FAD mice, scale bars: 100 μm. (B) Quantification of the area (%) covered by ThioS-positive amyloid plaques in cortex revealed a significantly higher plaque load with increased age. Cortical plaque load correlated significantly positive with (C) CSF NfL concentration and (D) serum NfL concentration when assessed over all age groups. Data are presented as median and IQR. Whiskers represent data within 1.5 IQR of the lower and upper quartiles. For comparison between groups, statistical analysis was performed using the Jonckheere-Terpstra trend test followed by the Mann-Whitney *U*-test for post hoc group comparisons between the youngest group an all other groups. *p*-values were corrected for multiple comparisons using the Bonferroni method (***$p < 0.00033$). Correlation analysis was performed using Spearman's rank-ordered correlation coefficient (***$p < 0.001$). Abbreviations: CSF, cerebrospinal fluid; IQR, interquartile range; NfL, neurofilament light; ThioS, thioflavin S.

the concentration of NfL in both CSF and blood has shown to remain stable over the 2 freeze-thaw cycles to which our samples have been exposed to (Keshavan et al., 2018; Koel-Simmelink et al., 2013; Vinter et al., 2020), differences in the effect of other pre-analytical factors that yet have not been investigated may have contributed to these results. Our finding that the NfL concentration in CSF may be significantly changed at an earlier time point than in plasma is in agreement with a previous study on sporadic AD (Pereira et al., 2017). However, the relationship between CSF and plasma NfL may be different in autosomal-dominant AD, as a recent study using the Dominantly Inherited Alzheimer Network cohort showed that the concentrations of NfL in both CSF and serum were significantly increased in mutation carriers compared to non-mutation carriers at approximately the same time, 6.8 years before the estimated symptom onset (Preische et al., 2019).

Comparisons between the groups also revealed that the concentration of NfL in both CSF and plasma was higher in patients with MCI categorized as A−N− when compared to A−N− CU subjects. The pathophysiology of MCI is multifactorial and may, in addition to accumulation of Aβ and gray matter degeneration, be associated with vascular damage and cerebrovascular disease resulting in compromised white matter integrity (Roberts et al., 2013). Indeed, the global white matter lesion burden in A−N− MCI patients was significantly higher than in A−N− CU subjects, and correlated with the concentration of NfL in both CSF and plasma (see Supplementary Fig. 6A–C). As NfL is particularly abundant in large myelinated axons that constitute the cerebral white matter, this may to some extent explain the increased NfL concentration in CSF and plasma in this group.

Evaluation of the diagnostic accuracy of NfL in CSF and plasma showed that the performance of NfL in CSF in distinguishing A−N− CU subject from A ± N+ CU subjects was fair. This was in contrast to NfL in plasma, where the separation between the groups was rather poor.

Given the translational importance of well-characterized mouse models in AD research, we further investigated if our findings in humans could be replicated in the 5×FAD mouse model of AD. Indeed, we found a positive correlation between NfL in CSF and serum in both 5×FAD and non-tg mice when assessed over all age groups, further supporting a likely CNS origin of NfL in blood. Importantly, in 5×FAD mice, the concentration of NfL in CSF was around 15 times higher compared to non-tg littermates already at 2 months of age, the time point at which myelin abnormalities and decreased axonal caliber have been reported (Gu et al., 2018), and the first extracellular Aβ plaques start to accumulate in the brain (Oakley et al., 2006). This was in contrast to NfL in serum, where increased concentrations were observed from 4 months of age. This coincides with the development of spatial memory deficits (Oakley et al., 2006), supporting our clinical findings that NfL in blood might be a reliable marker of axonal injury and loss first in the early symptomatic stage of AD. Our results are in agreement with previous studies in animal models of neurodegenerative diseases, in which the concentration of NfL in CSF was increased over wild-type controls at an earlier

time point than NfL in blood (Bacioglu et al., 2016; Soylu-Kucharz et al., 2017).

To reach the circulatory system, NfL and other proteins derived from the CNS must cross the blood-brain barrier (BBB). Although conflicting results have been reported, there has been some evidence of compromised BBB integrity in patients with MCI (Montagne et al., 2015) and AD dementia (Janelidze et al., 2017; Skillbäck et al., 2017), as well as in mouse models of Aβ pathology (Montagne et al., 2017). Even if no association has been found between blood NfL concentration and CSF/serum albumin ratio, the most established fluid biomarker for BBB function (Kalm et al., 2017), it is possible that significant leakage of NfL from the CNS into the blood initially occurs in the symptomatic stage of the disease. Hence, in addition to differences in variability, one may speculate that this to some extent contributes to our findings that NfL in blood is significantly increased at a later time point than in CSF. However, further studies are necessary to better understand the driving factors behind these differences.

4.2. NfL in relation to Aβ pathology

The concentration of NfL in CSF was elevated in subjects with Aβ pathology in all diagnostic groups, including CU subjects. This was in contrast to plasma NfL concentration, which was only increased in Aβ-positive MCI and AD dementia subject. When further investigating the association between NfL and the accumulation of Aβ in the brain, as measured by ^{18}F-flutemetamol PET, higher concentration of NfL in CSF was associated with greater Aβ plaque load in widespread cortical regions in CU subjects when uncorrected for multiple comparisons. However, associations between the concentration of plasma NfL and Aβ plaque load were more limited in this group. Similarly, in 5×FAD mice, the correlation with cortical plaque load was greater for the concentration of NfL in CSF compared with serum. Together, these results imply that NfL in CSF, but not in plasma, is a biomarker sensitive to biological processes related to Aβ pathology in the preclinical stages of sporadic AD. Surprisingly, neither NfL in CSF nor plasma was associated with the accumulation of Aβ in patients with MCI, which might be due to increased NfL concentrations caused by neurodegeneration independent of Aβ pathology in this heterogeneous group of patients.

Our findings that the concentration of NfL in CSF was related to Aβ positivity in the preclinical stage of sporadic AD is in agreement with previous reports (Bos et al., 2019; Pereira et al., 2017). Notably, by using the Alzheimer's Disease Neuroimaging Initiative cohort, Pereira and colleagues showed that the concentration of NfL in CSF was elevated and associated with brain atrophy already in CU subjects with pathological CSF Aβ42 levels. In line with the results from the present study, they also found that plasma NfL was increased and associated with brain atrophy only in symptomatic individuals (Pereira et al., 2017). Our results regarding plasma NfL are further supported by additional studies where no differences in plasma NfL concentrations between Aβ-positive and Aβ-negative CU subjects were reported, however, those studies did not investigate NfL in CSF (Chatterjee et al., 2018; Mattsson et al., 2017). Moreover, in a study population consisting of mainly CU subjects, Mielke and colleagues found no association between baseline plasma NfL concentration and baseline or longitudinal changes in global cortical amyloid burden as determined by PiB-PET. Nevertheless, similar results were obtained for baseline CSF NfL concentration (Mielke et al., 2019).

4.3. NfL in relation to white matter changes

Increased concentrations of NfL in body fluids are thought to reflect injury and loss of large myelinated axons, which are predominately found within the cerebral white matter (Khalil et al., 2018). Although AD has traditionally been viewed as a disease of the gray matter (Amlien and Fjell, 2014), several studies employing neuroimaging modalities have provided evidence of both macro- and microstructural white matter abnormalities during the course of the disease (Agosta et al., 2011; Liu et al., 2009; Mayo et al., 2017; Medina et al., 2006; Nasrabady et al., 2018). Indeed, it has been reported that the concentration of NfL in CSF, but not in plasma, correlates with white matter macrostructural changes in patients with MCI and AD dementia (Mattsson et al., 2017; Zetterberg et al., 2016). Furthermore, in CU subjects and prodromal AD, associations between NfL in CSF and DTI measurements of white matter microstructure were recently described (Moore et al., 2018). These findings are in line with those from the present study, in which the concentration of NfL in CSF was negatively associated with FA and positively associated with MD in widespread white matter regions, suggesting that increased concentration of NfL in CSF reflect increased white matter damage (Gold et al., 2012). In contrast, the concentration of NfL in plasma associated with FA only in patients with MCI, whereas no association with MD was found in any of the diagnostic groups. To our knowledge, this is the first study to investigate associations between plasma NfL and white matter microstructural changes measured by DTI. Our findings suggest that NfL in CSF may predict white matter damage at an earlier stage of sporadic AD compared to NfL in plasma.

4.4. Limitations

A limitation of our study is the use of a cross-sectional study design, which did not allow us to study changes in the concentrations of NfL in CSF compared to serum over time. Longitudinal studies with serial measurements would be needed to further assess the use of NfL in CSF in comparison to plasma as a biomarker of axonal injury and loss in preclinical sporadic AD. In addition, categorization based on A/N status resulted in a relatively small sample size in some of the groups, reducing the power of the study.

In the present study, we made use of the 5×FAD mouse model of AD. These mice have an aggressive disease presentation and progression, with accumulation of Aβ plaques starting already at 2 months of age. As CSF and serum were collected from this time point, it was not possible to study potential changes in NfL prior to plaque deposition. Thus, in order to get a better understanding as to when the concentrations of NfL starts to increase in the early stage of the disease, our findings should be replicated in additional mouse models with a slower disease progression, more similar to that in humans. Furthermore, the overexpression of APP in 5×FAD mice results in subsequent overproduction of APP fragments other than Aβ (Sasaguri et al., 2017). These fragments, rather than Aβ, might contribute to pathological changes related to the release of NfL into CSF and blood. To overcome this issue, the use of recently developed APP KI mice (Saito et al., 2014) would be preferable over first-generation tg mouse models for future studies.

5. Conclusion

In conclusion, our findings suggest that NfL concentration in CSF might be a useful biomarker for assessment of axonal injury and loss already in preclinical sporadic AD, whereas NfL concentration in plasma may be reliable for similar pathological processes somewhat later, that is, during the early symptomatic stages of the disease. Furthermore, 5×FAD mice may be a valuable model for future experimental studies on the underlying mechanisms for changes in NfL in CSF and blood in AD, as well as on treatment responses to novel disease-modifying drugs.

Disclosure

E. Andersson, S. Janelidze, B. Lampinen, M. Nilsson, A. Leuzy, and E. Stomrud report no disclosure. O. Hansson has acquired research support (for the institution) from Roche, GE Healthcare, Biogen, AVID Radiopharmaceuticals, and Euroimmun. In the past 2 years, he has received consultancy/speaker fees (paid to the institution) from Biogen and Roche. H. Zetterberg has served at scientific advisory boards for Roche Diagnostics, Wave, Samumed, and CogRx, and has given lectures in symposia sponsored by Biogen and AlzeCure. K. Blennow has served as a consultant or at advisory boards for Alector, Biogen, CogRx, Lilly, MagQu, Novartis, and Roche Diagnostics. H. Zetterberg and K. Blennow are co-founders of Brain Biomarker Solutions in Gothenburg AB, a GU Ventures-based platform company at the University of Gothenburg.

CRediT authorship contribution statement

Emelie Andersson: Formal analysis, Investigation, Writing - original draft, Visualization. **Shorena Janelidze:** Formal analysis, Investigation, Writing - review & editing. **Björn Lampinen:** Formal analysis, Visualization, Writing - review & editing. **Markus Nilsson:** Formal analysis, Visualization, Writing - review & editing. **Antoine Leuzy:** Formal analysis, Visualization, Writing - review & editing. **Erik Stomrud:** Investigation, Writing - review & editing. **Kaj Blennow:** Methodology, Investigation, Writing - review & editing. **Henrik Zetterberg:** Methodology, Investigation, Writing - review & editing. **Oskar Hansson:** Conceptualization, Validation, Writing - review & editing, Supervision, Project administration, Funding acquisition.

Acknowledgements

Work at the authors' research center was supported by the European Research Council (grant no. 311292), the Swedish Research Council (grant no. 2016-00906), the Knut and Alice Wallenberg foundation (grant no. 2017-0383), the Marianne and Marcus Wallenberg foundation (grant no. 2015.0125), the Strategic Research Area MultiPark (Multidisciplinary Research in Parkinson's disease) at Lund University, the Swedish Alzheimer Foundation (grant no. AF-745911), the Swedish Brain Foundation (grant no. FO2019-0326), The Parkinson foundation of Sweden (grant no. 1127718), The Parkinson Research Foundation, the Skåne University Hospital Foundation (grant no. 2019-o000032), and the Swedish federal government under the ALF agreement (grant no. 2018-Projekt0279). Doses of ^{18}F-flutemetamol injections were sponsored by GE Healthcare.

Appendix A. Supplementary data

Supplementary data associated with this article can be found, in the online version, at https://doi.org/10.1016/j.neurobiolaging.2020.07.018.

References

Agosta, F., Pievani, M., Sala, S., Geroldi, C., Galluzzi, S., Frisoni, G.B., Filippi, M., 2011. White matter damage in Alzheimer disease and its relationship to gray matter atrophy. Radiology 258, 853–863.

Amlien, I.K., Fjell, A.M., 2014. Diffusion tensor imaging of white matter degeneration in Alzheimer's disease and mild cognitive impairment. Neuroscience 276, 206–215.

Andersson, J.L.R., Jenkinson, M., Smith, S., 2007. Non-linear Registration aka Spatial Normalisation. FMRIB Technical Report (No. TR07JA2). FMRIB Analysis Group of the University of Oxford. FMRIB technical report.

Bacioglu, M., Maia, L.F., Preische, O., Schelle, J., Apel, A., Kaeser, S.A., Schweighauser, M., Eninger, T., Lambert, M., Pilotto, A., Shimshek, D.R., Neumann, U., Kahle, P.J., Staufenbiel, M., Neumann, M., Maetzler, W., Kuhle, J., Jucker, M., 2016. Neurofilament light chain in blood and CSF as marker of disease progression in mouse models and in neurodegenerative diseases. Neuron 91, 56–66.

Basser, P.J., Mattiello, J., Lebihan, D., 1994. MR diffusion tensor spectroscopy and imaging. Biophys. J. 66, 259–267.

Blennow, K., Hampel, H., Weiner, M., Zetterberg, H., 2010. Cerebrospinal fluid and plasma biomarkers in Alzheimer disease. Nat. Rev. Neurol. 6, 131–144.

Blennow, K., Zetterberg, H., 2018. Biomarkers for Alzheimer's disease: current status and prospects for the future. J. Intern. Med. 284, 643–663.

Bos, I., Vos, S., Verhey, F., Scheltens, P., Teunissen, C., Engelborghs, S., Sleegers, K., Frisoni, G., Blin, O., Richardson, J.C., Bordet, R., Tsolaki, M., Popp, J., Peyratout, G., Martinez-Lage, P., Tainta, M., Lleó, A., Johannsen, P., Freund-Levi, Y., Frölich, L., Vandenberghe, R., Westwood, S., Dobricic, V., Barkhof, F., Legido-Quigley, C., Bertram, L., Lovestone, S., Streffer, J., Andreasson, U., Blennow, K., Zetterberg, H., Visser, P.J., 2019. Cerebrospinal fluid biomarkers of neurodegeneration, synaptic integrity, and astroglial activation across the clinical Alzheimer's disease spectrum. Alzheimer's Dement. 15, 644–654.

Chatterjee, P., Goozee, K., Sohrabi, H.R., Shen, K., Shah, T., Asih, P.R., Dave, P., ManYan, C., Taddei, K., Chung, R., Zetterberg, H., Blennow, K., Martins, R.N., 2018. Association of plasma neurofilament light chain with neocortical amyloid-β load and cognitive performance in cognitively normal elderly participants. J. Alzheimer's Dis. 63, 479–487.

Desikan, R.S., Ségonne, F., Fischl, B., Quinn, B.T., Dickerson, B.C., Blacker, D., Buckner, R.L., Dale, A.M., Maguire, R.P., Hyman, B.T., Albert, M.S., Killiany, R.J., 2006. An automated labeling system for subdividing the human cerebral cortex on MRI scans into gyral based regions of interest. Neuroimage 31, 968–980.

Gold, B.T., Johnson, N.F., Powell, D.K., Smith, C.D., 2012. White matter integrity and vulnerability to Alzheimer's disease: preliminary findings and future directions. Biochim. Biophys. Acta 1822, 416–422.

Gu, L., Wu, D., Tang, X., Qi, X., Li, X., Bai, F., Chen, X., Ren, Q., Zhang, Z., 2018. Myelin changes at the early stage of 5XFAD mice. Brain Res. Bull. 137, 285–293.

Gustafson, D.R., Skoog, I., Rosengren, L., Zetterberg, H., Blennow, K., 2007. Cerebrospinal fluid beta-amyloid 1-42 concentration may predict cognitive decline in older women. J. Neurol. Neurosurg. Psychiatry 78, 461–464.

Hampel, H., O'Bryant, S.E., Molinuevo, J.L., Zetterberg, H., Masters, C.L., Lista, S., Kiddle, S.J., Batrla, R., Blennow, K., 2018. Blood-based biomarkers for Alzheimer disease: mapping the road to the clinic. Nat. Rev. Neurol. 14, 639–652.

Horsfield, M.A., Jones, D.K., 2002. Applications of diffusion-weighted and diffusion tensor MRI to white matter diseases—a review. NMR Biomed. 15, 570–577.

Jack, C.R., Bennett, D.A., Blennow, K., Carrillo, M.C., Dunn, B., Haeberlein, S.B., Holtzman, D.M., Jagust, W., Jessen, F., Karlawish, J., Liu, E., Molinuevo, J.L., Montine, T., Phelps, C., Rankin, K.P., Rowe, C.C., Scheltens, P., Siemers, E., Snyder, H.M., Sperling, R., 2018. NIA-AA Research Framework: toward a biological definition of Alzheimer's disease. Alzheimers. Dement. 14, 535–562.

Jack, C.R., Wiste, H.J., Weigand, S.D., Therneau, T.M., Lowe, V.J., Knopman, D.S., Gunter, J.L., Senjem, M.L., Jones, D.T., Kantarci, K., Machulda, M.M., Mielke, M.M., Roberts, R.O., Vemuri, P., Reyes, D.A., Petersen, R.C., 2017. Defining imaging biomarker cut points for brain aging and Alzheimer's disease. Alzheimer's Dement. 13, 205–216.

Janelidze, S., Hertze, J., Nägga, K., Nilsson, K., Nilsson, C., Wennström, M., van Westen, D., Blennow, K., Zetterberg, H., Hansson, O., 2017. Increased blood-brain barrier permeability is associated with dementia and diabetes but not amyloid pathology or APOE genotype. Neurobiol. Aging 51, 104–112.

Kalm, M., Boström, M., Sandelius, Å., Eriksson, Y., Ek, C.J., Blennow, K., Björk-Eriksson, T., Zetterberg, H., 2017. Serum concentrations of the axonal injury marker neurofilament light protein are not influenced by blood-brain barrier permeability. Brain Res. 1668, 12–19.

Keshavan, A., Heslegrave, A., Zetterberg, H., Schott, J.M., 2018. Blood-based biomarkers stability of blood-based biomarkers of Alzheimer's disease over multiple freeze-thaw cycles. Alzheimer's Dement. 10, 448–451.

Khalil, M., Teunissen, C.E., Otto, M., Piehl, F., Sormani, M.P., Gattringer, T., Barro, C., Kappos, L., Comabella, M., Fazekas, F., Petzold, A., Blennow, K., Zetterberg, H., Kuhle, J., 2018. Neurofilaments as biomarkers in neurological disorders. Nat. Rev. Neurol. 14, 577–589.

Klein, S., Staring, M., Murphy, K., Viergever, M.A., Pluim, J., 2010. Elastix: a toolbox for intensity-based medical image registration. IEEE Trans. Med. Imaging 29, 196–205.

Koel-Simmelink, M.J.A., Vennegoor, A., Killestein, J., Blankenstein, M.A., Norgren, N., Korth, C., Teunissen, C.E., 2013. The impact of pre-analytical variables on the stability of neurofilament proteins in CSF, determined by a novel validated SinglePlex Luminex assay and ELISA. J. Immunol. Methods 402, 43–49.

Laforce, R., Soucy, J.P., Sellami, L., Dallaire-Théroux, C., Brunet, F., Bergeron, D., Miller, B.L., Ossenkoppele, R., 2018. Molecular imaging in dementia: past, present, and future. Alzheimer's Dement. 14, 1522–1552.

Liu, L., Duff, K., 2008. A technique for serial collection of cerebrospinal fluid from the cisterna magna in mouse. JoVE 21, 960.

Liu, Y., Spulber, G., Lehtimäki, K.K., Könönen, M., Hallikainen, I., Gröhn, H., Kivipelto, M., Hallikainen, M., Vanninen, R., Soininen, H., 2009. Diffusion tensor imaging and tract-based spatial statistics in Alzheimer's disease and mild cognitive impairment. Neurobiol. Aging 32, 1558–1571.

Lundqvist, R., Lilja, J., Thomas, B.A., Lötjönen, J., Villemagne, V.L., Rowe, C.C., Thurfjell, L., 2013. Implementation and validation of an adaptive template registration method for 18F-flutemetamol imaging data. J. Nucl. Med. 54, 1472–1478.

Lee, V.M.-Y., Carden, M.J., Schlaepfer, W.W., 1986. Structural similarities and differences between neurofilament proteins from five different species as revealed using monoclonal antibodies. J. Neurosci. 6, 2179–2186.
Mattsson, N., Andreasson, U., Zetterberg, H., Blennow, K., 2017. Association of plasma neurofilament light with neurodegeneration in patients with Alzheimer disease. JAMA Neurol. 74, 557–566.
Mattsson, N., Cullen, N.C., Andreasson, U., Zetterberg, H., Blennow, K., 2019. Association between longitudinal plasma neurofilament light and neurodegeneration in patients with Alzheimer disease. JAMA Neurol. 76, 791–799.
Mayo, C.D., Mazerolle, E.L., Ritchie, L., Fisk, J.D., Gawryluk, J.R., 2017. Longitudinal changes in microstructural white matter metrics in Alzheimer's disease. Neuroimage Clin. 13, 330–338.
Mckhann, G.M., Knopman, D.S., Chertkow, H., Hyman, B.T., Jack, C.R., Kawas, C.H., Klunk, W.E., Koroshetz, W.J., Manly, J.J., Mayeux, R., Mohs, R.C., Morris, J.C., Rossor, M.N., Scheltens, P., Carrillo, M.C., Thies, B., Weintraub, S., Phelps, C.H., 2011. The diagnosis of dementia due to Alzheimer's disease: recommendations from the National Institute on Aging-Alzheimer's Association workgroups on diagnostic guidelines for Alzheimer's disease. Alzheimer's Dement. 7, 263–269.
Medina, D., Detoledo-Morrell, L., Urresta, F., Gabrieli, J.D.E., Moseley, M., Fleischman, D., Bennett, D.A., Leurgans, S., Turner, D.A., Stebbins, G.T., 2006. White matter changes in mild cognitive impairment and AD: a diffusion tensor imaging study. Neurobiol. Aging 27, 663–672.
Meng, X.-L., Rosenthal, R., Rubin, D.B., 1992. Comparing correlated correlation coefficients. Psychol. Bull. 111, 172–175.
Mielke, M.M., Neurology, S.K., Mielke, M.M., Radiology, R.C.P., 2019. Plasma and CSF neurofilament light relation to longitudinal neuroimaging and cognitive measures. Neurology 93, e252–e260.
Montagne, A., Barnes, S.R., Law, M., Zlokovic Correspondence, B.V., Sweeney, M.D., Halliday, M.R., Sagare, A.P., Zhao, Z., Toga, A.W., Jacobs, R.E., Liu, C.Y., Amezcua, L., Harrington, M.G., Chui, H.C., Zlokovic, B.V., 2015. Blood-brain barrier breakdown in the aging human hippocampus. Neuron 85, 296–302.
Montagne, A., Zhao, Z., Zlokovic, B.V., 2017. Alzheimer's disease: a matter of blood-brain barrier dysfunction? J. Exp. Med. 214, 3151–3169.
Moore, E.E., Hohman, T.J., Badami, F.S., Pechman, K.R., Osborn, K.E., Acosta, L.M.Y., Bell, S.P., Babicz, M.A., Gifford, K.A., Anderson, A.W., Goldstein, L.E., Blennow, K., Zetterberg, H., Jefferson, A.L., 2018. Neurofilament relates to white matter microstructure in older adults. Neurobiol. Aging 70, 233–241.
Nasrabady, S.E., Rizvi, B., Goldman, J.E., Brickman, A.M., 2018. White matter changes in Alzheimer's disease: a focus on myelin and oligodendrocytes. Acta Neuropathol. Commun. 6, 1–10.
Oakley, H., Cole, S.L., Logan, S., Maus, E., Shao, P., Craft, J., Guillozet-Bongaarts, A., Ohno, M., Disterhoft, J., Van Eldik, L., Berry, R., Vassar, R., 2006. Intraneuronal beta-amyloid aggregates, neurodegeneration, and neuron loss in transgenic mice with five familial Alzheimer's disease mutations: potential factors in amyloid plaque formation. J. Neurosci. 26, 10129–10140.
Olsson, B., Portelius, E., Cullen, N.C., Sandelius, Å., Zetterberg, H., Andreasson, U., Höglund, K., Irwin, D.J., Grossman, M., Weintraub, D., Chen-Plotkin, A., Wolk, D., McCluskey, L., Elman, L., Shaw, L.M., Toledo, J.B., McBride, J., Hernandez-Con, P., Lee, V.M.-Y., Trojanowski, J.Q., Blennow, K., 2019. Association of cerebrospinal fluid neurofilament light protein levels with cognition in patients with dementia, motor neuron disease, and movement disorders. JAMA Neurol. 76, 318–325.
Pereira, J.B., Westman, E., Hansson, O., 2017. Association between cerebrospinal fluid and plasma neurodegeneration biomarkers with brain atrophy in Alzheimer's disease. Neurobiol. Aging 58, 14–29.
Preische, O., Schultz, S.A., Apel, A., Kuhle, J., Kaeser, S.A., Barro, C., Gräber, S., Kuder-Buletta, E., LaFougere, C., Laske, C., Vöglein, J., Levin, J., Masters, C.L., Martins, R., Schofield, P.R., Rossor, M.N., Graff-Radford, N.R., Salloway, S., Ghetti, B., Ringman, J.M., Noble, J.M., Chhatwal, J., Goate, A.M., Benzinger, T.L.S., Morris, J.C., Bateman, R.J., Wang, G., Fagan, A.M., McDade, E.M., Gordon, B.A., Jucker, M., Dominantly Inherited Alzheimer Network, 2019. Serum neurofilament dynamics predicts neurodegeneration and clinical progression in presymptomatic Alzheimer's disease. Nat. Med. 25, 277–283.
Roberts, R., Ch B, Knopman, D.S., 2013. Classification and epidemiology of MCI. Clin. Geriatr. Med. 29, 753–772.
Saito, T., Matsuba, Y., Mihira, N., Takano, J., Nilsson, P., Itohara, S., Iwata, N., Saido, T.C., 2014. Single App knock-in mouse models of Alzheimer's disease. Nat. Neurosci. 17, 661–663.
Sakaguchi, T., Okada, M., Kitamura, T., Kawasaki, K., 1993. Reduced diameter and conduction velocity of myelinated fibers in the sciatic nerve of a neurofilament-deficient mutant quail. Neurosci. Lett. 153, 65–68.
Sasaguri, H., Nilsson, P., Hashimoto, S., Nagata, K., Saito, T., De Strooper, B., Hardy, J., Vassar, R., Winblad, B., Saido, T.C., 2017. APP mouse models for Alzheimer's disease preclinical studies. EMBO J. 36, 2473–2487.
Schmidt, P., Gaser, C., Arsic, M., Buck, D., Förschler, A., Berthele, A., Hoshi, M., Ilg, R., Schmid, V.J., Zimmer, C., Hemmer, B., Mühlau, M., 2012. An automated tool for detection of FLAIR-hyperintense white-matter lesions in multiple sclerosis. Neuroimage 59, 3774–3783.
Skillbäck, T., Delsing, L., Synnergren, J., Mattsson, N., Janelidze, S., Nägga, K., Kilander, L., Hicks, R., Wimo, A., Winblad, B., Hansson, O., Blennow, K., Eriksdotter, M., Zetterberg, H., 2017. CSF/serum albumin ratio in dementias: a cross-sectional study on 1861 patients. Neurobiol. Aging 59, 1–9.
Skoog, I., Davidsson, P., Aevarsson, Ó., Vanderstichele, H., Vanmechelen, E., Blennow, K., 2003. Cerebrospinal fluid beta-amyloid 42 is reduced before the onset of sporadic dementia: a population-based study in 85-year-olds. Dement. Geriatr. Cogn. Disord. 15, 169–176.
Smith, S.M., Jenkinson, M., Johansen-Berg, H., Rueckert, D., Nichols, T.E., Mackay, C.E., Watkins, K.E., Ciccarelli, O., Cader, M.Z., Matthews, P.M., Behrens, T.E.J., 2006. Tract-based spatial statistics: voxelwise analysis of multi-subject diffusion data. Neuroimage 31, 1487–1505.
Soylu-Kucharz, R., Sandelius, Å., Sjögren, M., Blennow, K., Wild, E.J., Zetterberg, H., Björkqvist, M., 2017. Neurofilament light protein in CSF and blood is associated with neurodegeneration and disease severity in Huntington's disease R6/2 mice. Sci. Rep. 7, 14114.
Stomrud, E., Hansson, O., Blennow, K., Minthon, L., Londos, E., 2007. Cerebrospinal fluid biomarkers predict decline in subjective cognitive function over 3 years in healthy elderly. Dement. Geriatr. Cogn. Disord. 24, 118–124.
Vinter, C., Hviid, B., Knudsen, C.S., Parkner, T., 2020. Reference interval and pre-analytical properties of serum neurofilament light chain in Scandinavian adults. Scand. J. Clin. Lab. Invest. 80, 291–295.
Yuan, A., Rao, M.V., Veeranna, Nixon, R.A., 2017. Neurofilaments and neurofilament proteins in health and disease. Cold Spring Harb. Perspect. Biol. 9, a018309.
Zetterberg, H., Skillbäck, T., Mattsson, N., Trojanowski, J.Q., Portelius, E., Shaw, L.M., 2016. Association of cerebrospinal fluid neurofilament light concentration with Alzheimer disease progression. JAMA Neurol. 73, 60–67.
Zhu, Q., Couillard-Després, S., Julien, J.-P., 1997. Delayed maturation of regenerating myelinated axons in mice lacking neurofilaments. Exp. Neurol. 148, 299–316.